

Mathematical modeling & design of worm and worm gear pair for determining the surface stress acting on the tooth of worm and worm gear for plug Valve application

Yuvraj B. Jadhava, Abhijeet P. Shahb

Abstract- Gears are one of the most important components in mechanical power transmission system. The bending stress and contact stresses of gear tooth is regarded as one of the key contributor for the failure of the gear in the gear set. Thus the analysis for these stresses has become essential for minimizing the chance of failure and optimized design of the gear. A worm gear, used in many industrial applications, can provide substantially increasing output torque due to its high gear ratio. It occupies small space due to its compactness. These advantages are very much appealing to automotive manufacturers in particular, as they are moving from the Hydraulic Power Steering to the Electric Power Steering system to provide assistant torque to the driver. The worm gear has great potential application in actuation of various types of valves, in various machineries and instruments.. This paper focuses on design of worm and worm gear, developing mathematical model of gear. This paper gives in detail design procedure for the worm and worm gear in plug valve application. The mathematical model of worm gear in plug valve application is developed to determine the Surface stresses acting on the tooth gear. The expression is obtained by using the maximum-shear-stress distribution in order to know the maximum-shear-stress value. The obtained results in this paper provides significant information for predicting the static and dynamic performance of worm gear pairs.

Keywords:Worm gear; Plug valve; Surface stress; gear design; Hertzian contact stress; Flamant generalized stress equation

1. INTRODUCTION

A worm gear is widely used in many industrial applications, can provide substantially increasing output torque due to its high gear ratio. It occupies small space due to its compactness. These advantages are very appealing to automotive manufacturers in particular, as they are moving from the HPS to the EPS system to provide assistant torque to the driver. Plug valves are valves with cylindrical or conically tapered "plugs" which can be rotated inside the valve body to control flow through the valve. The plugs in plug valves have one or more hollow passageways going sideways through the plug, so that fluid can flow

through the plug when the valve is open. Use of worm & worm gear pair for plug valve application provide a considerable mechanical advantage so that a given applied force must be able to overcome a comparatively high resisting force, which enhance the plug valve actuation, and reduce the human work for actuation.

This paper presents a design & mathematical model of worm gear in plug valve is to be developed to determine the surface stresses acting on the tooth gear. The new expression is obtained by using the maximum-shear-stress distribution in order to know the maximum-shear-stress value.

-
- Author name is currently pursuing masters degree program in electric power engineering in University, Country, PH-01123456789. E-mail: author_name@mail.com
 - Co-Author name is currently pursuing masters degree program in electric power engineering in University, Country, PH-01123456789. E-mail: author_name@mail.com
- (This information is optional; change it according to your need.)

Table 1.Strength Rating Factors

Parameters	Values	Parameters	values	Parameters	Values
Velocity ratio (V.R.)	5	Diametral Quotient (q)	10	Clearance (C)	0.8633mm
Number of starts on worm (Z ₂)	6	Centre distance (a)	100 mm	Deddendum (h _{f1})	49 mm
Normal pressure angle (ψ _r)	25	Pitch circle diameter of worm (D ₁)	50mm.	Pitch circle diameter of worm wheel (D ₂)	150mm
Teeth on Worm Wheel(Z ₁)	30	Outside diameter of worm (D _{a1})	60mm	Throat diameter of worm wheel (D _{a2})	157.26 mm
Lead Angle of Worm(λ)	30.31°	Root diameter of worm. (D _{f1})	41mm.	Root diameter of worm wheel (D _{f2})	141.72 mm
Helix Angle of Worm Wheel (φ)	30.31°	Axial pitch of worm (P _x)	15.70mm	Face Width (b)	36.5 mm
Helix Angle of Worm (γ)	59.69°	Addendum (h _{a1})	5mm	Lead of Worm (L)	15.70 mm

2. DESIGN OF WORM & WORM WHEEL

By using the design procedure of worm and worm

2.1. MATERIAL SELECTION.

Worm Material

10C4, 14C4 (Case Hardened steel)

$$S_{ut} = 980 \text{ N/mm}^2$$

BHN = 255

$$\sigma_{allowable} = 326.66 \text{ N/mm}^2$$

Worm Wheel Material

ASTM- A535/88-55-06 (Ductile iron)

$$S_{ut} = 275 \text{ N/mm}^2$$

gear we find out different values of gears parameters.

Which shown in table no. 1.

$$\text{BHN} = 255$$

$$\sigma_{allowable} = 91.66 \text{ N/mm}^2$$

2.2. STRENGTH OF WORM GEAR TEETH.

We know that for 30 involute teeth from Lewis factor

(y') :

$$y' = 0.358$$

Check for Tangential Load Transmitted (FT)

$$FT = \sigma b \times C_v \times b \times \pi \times m \times y' = 17391.44 \text{ N}$$

Power transmitted due to tangential load (PT)

$$PT = \frac{F \times V}{1000} = 5.04 \text{ kW}$$

Since this is more than the power to be transmitted,
DESIGN IS SAFE

- Check for Dynamic Load (FD)

$$FD = \frac{F_t}{C.V} = 18813.76 \text{ N}$$

Power transmitted due to dynamic load (PD)

$$PD = \frac{Fd \times V}{1000} = 5.45 \text{ kW}$$

Since this is more than the power to be transmitted,
DESIGN IS SAFE.

Check for Static Load

Flexural Endurance limit (Fc)

$$F_c = 1.75(\text{BHN}) = 1.75(255) = 446.25 \text{ N/mm}^2$$

Static load (Fs)

$$F_s = F_c \times b \times \pi \times m \times y' = 91595.47 \text{ N}$$

Power transmitted due to static load (PS)

$$PS = \frac{F_s \times V}{1000} = 26.56 \text{ kW}$$

Since this is more than the power to be transmitted,
DESIGN IS SAFE.

Input speed of worm (Nw) = 190 rpm

Output speed of worm (Ng) $= \frac{N_w}{V.R} = \frac{190}{5} = 38 \text{ rpm}$

Pitch Line Velocity of Worm (V₁)

$$V_1 = \frac{\pi \times D_1 \times N_1}{60000} = 0.49 \text{ m/s}$$

Pitch Line Velocity of Worm Wheel (V₂)

$$V_2 = \frac{\pi \times D_2 \times N_2}{60000} = 0.29 \text{ m/s}$$

Rubbing velocity (V_s)

$$V_s = \frac{\pi \times D_1 \times N_1}{60000 \times \cos \alpha} = 0.5761 \text{ m/s}$$

Velocity Factor (CV)

$$C_v = \frac{6}{6+v} = 0.9244$$

From fig. 1 of coefficient of friction v/s rubbing speed,
we find that the coefficient of friction

Corresponding to rubbing velocity of 0.57 m/s =
0.051(μ)

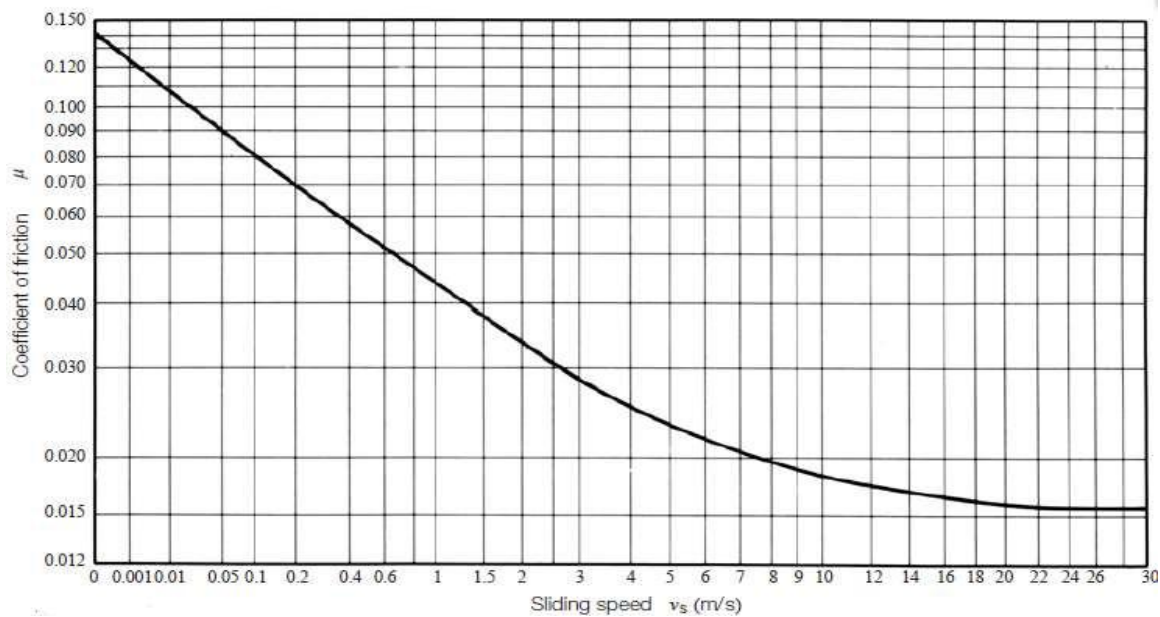


Fig. 1. Coefficient of Friction.[10]

Friction Angle (ϕF)

$$\phi F = \tan^{-1}(\mu) = 2.9195^\circ$$

Overall Efficiency of Worm and Worm Wheel (η)

$$\eta = \frac{\tan \lambda}{\tan(\lambda + \phi F)} = 0.8812 = 88\%$$

3. 2.3. SELF-LOCKING OR OVER-RUNNING

$$\mu < \cos \psi_r * \tan \phi$$

Where,

μ - Coefficient of friction between the worm and the gear.

ψ_r - is the pressure angle of the gear train

ϕ - Helix angle of the worm.

So,

$$0.051 < 0.07546$$

Thus the system is "self-locking"

4. MATHEMATICAL MODELING

Contact process between worm gear and worm wheel is comparable with the two cylinders with the same radius of curvature loaded in rolling contact. Based in such comparison, the contact between two cylinders produced in loading can be solved by using Hertzian polynomial equation, Elasticity theory & The Flamant generalized stress equation to determine the pressure distribution and to calculate the state of stresses beneath the contact surface. By using the state of stresses equations, we can calculate the maximum-shear-stress distribution in gear tooth contact surface.

In this mathematical model worm and worm gear are considered as two sphere and stresses are calculated by the pressure distribution on gear and pinion in contact area.

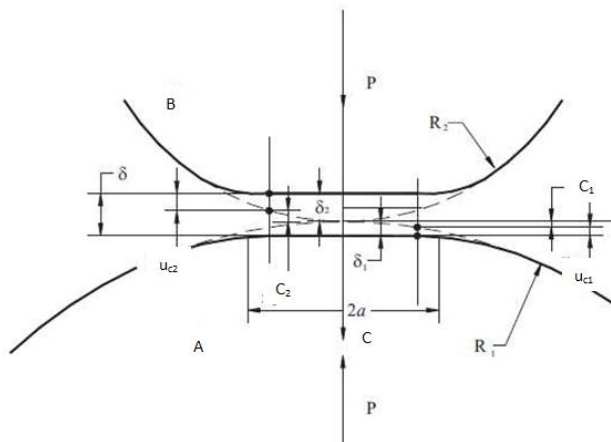


Fig. 2. The contact phenomenon between the teeth of gear and pinion [12]

Fig. 1 shows Pinion and gear tooth in contact under the action of a load P. Dashed lines show the original shape of the two bodies and the continuous lines shows their shapes under the load P. From Figure, the gear and pinion tooth profile radii are R2 and R1 resp., and the strip of the contact area is 2a. Then, from the scheme the relative elastic displacements for each tooth surface can be expressed as

$$u_{c1} + u_{c2} = \delta - c_1 - c_2 \quad (1)$$

Where u_{c1} and u_{c2} are the displacements of any points over the contact surface of body A and body B respectively, the total body displacement and c_1 and c_2 the positions of the points over the contact surface. The Hertzian expressions whose plots approaches to each tooth circular convexities on the contact surface are;

$$C_1 = \frac{X_1^2}{2R_1} \quad \text{and} \quad C_2 = \frac{X_2^2}{2R_2} \quad (2)$$

At certain point in the contact surface $x_1 = x_2 = x$; then, substituting Equations (2) into Equation (1) and by making

$$\frac{1}{R_1} + \frac{1}{R_2} = \frac{1}{R} \quad (3)$$

it is obtained

$$u_{c1} + u_{c2} = u_c = \delta - \frac{X^2}{2R} \quad (4)$$

This is the displacement equation for the any point in the contact. Then, the variation of the contact surface along the x-direction can be determined by partial differentiation of Equation (4) with respect to x, resulting in

$$\frac{\delta u_c}{\delta X} = -\frac{X}{R} \quad (5)$$

3.1 DISPLACEMENTS PRODUCED BY THE PRESSURE DISTRIBUTION ON CONTACT AREA

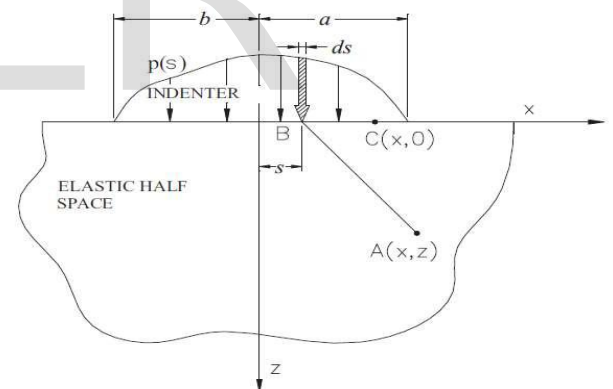


Fig. 3. Normal pressure distribution over an elastic half-space [12]

The load acting on the surface at B, distance s of O, on an elemental area of width ds can be assumed as a concentrated normal force P of magnitude $p(s)ds$ acting at B. The state of stresses produced by P at point A, are calculated using Flamant equation:

$$\sigma_r = -\frac{2P \cos \theta}{\pi r}$$

This equation in rectangular coordinates become

$$\begin{aligned}\sigma_x &= \sigma_r \sin^2 \theta = -\frac{2P}{\pi} \frac{x^2 z}{(x^2 + z^2)^2} \\ \sigma_z &= \sigma_r \cos^2 \theta = -\frac{2P}{\pi} \frac{z^3}{(x^2 + z^2)^2}\end{aligned}$$

(6)

$$\tau_{zx} = \sigma_r \sin \theta \cos \theta = -\frac{2P}{\pi} \frac{xz^2}{(x^2 + z^2)^2}$$

Using Equations (6), replacing x by x s to relocate each point to the origin and integrating over the loaded region, b < s < a, we get,

$$\begin{aligned}\sigma_x &= -\frac{2Z}{\pi} \int_{-b}^a \frac{p(s)(x-s)^2 ds}{[(x-s)^2 + z^2]^2} \\ \sigma_z &= -\frac{2z^3}{\pi} \int_{-b}^a \frac{p(s) ds}{[(x-s)^2 + z^2]^2} \\ \sigma_{zx} &= -\frac{2z^2}{\pi} \int_{-b}^a \frac{p(s)(x-s) ds}{[(x-s)^2 + z^2]^2}\end{aligned}$$

(7)

These are the basis equations to determine the maximum-shear-stress.

For the displacements of points over the contact surface and the distortion under the load action, the Hook's law and the Flamant equation are used, which results in

$$\begin{aligned}\frac{\partial u_r}{\partial r} &= \frac{(1-\nu^2)}{E} \frac{2P}{\pi} \frac{\cos \theta}{r} \\ \frac{1}{r} \frac{\partial u_\theta}{\partial \theta} + \frac{\partial u_\theta}{\partial r} - \frac{u_\theta}{r} &= \frac{Tr_\theta}{G} = 0\end{aligned}$$

After integration, the displacements can be obtained (as derived by Tim-oshenko & Goodier [12])

$$[u_r]_{\theta=\frac{\pi}{2}} = [u_r]_{\theta=-\frac{\pi}{2}} = -\frac{(1-2\nu)(1+\nu)P}{2E}$$

$$[u_\theta]_{\theta=\frac{\pi}{2}} = -[u_\theta]_{\theta=-\frac{\pi}{2}} = \frac{(1-\nu^2)}{\pi E} 2P \ln \frac{r_\theta}{r} - \frac{(1-\nu)}{\pi E} P$$

Solving integral we find

$$p(X) = -\frac{E^*}{2\pi a R (1-X^2)^{1/2}} \int_{-1}^1 \frac{(1-S^2)^{1/2}}{X-S} S dS + \frac{P}{\pi a (1-X^2)^{1/2}}$$

(9)

Now, in order to restrict the action of the pressure distribution into the loaded area we make p(X) = 0 at X = ±1 in Equation (9), in this way

$$P = \frac{\pi a^2 E}{4R}$$

(10)

Where, a = $\sqrt{\frac{4RP}{\pi E}}$

(10.1)

Taking into account that p(X) reaches its maximum value at X = 0 and that p(X) = p(0) = p₀, from Equation (9) we can get also

$$P_0 = \frac{2P}{\pi a}$$

(11)

Finally, substituting Equations (10) and (11) into Equation (9) and the principal value of the integral, we arrive to the Hertzian pressure distribution

$$P(x) = P_0 (1 - x^2)^{1/2}$$

(12) $P(x) = P_0 (1 - \frac{x^2}{a^2})^{1/2}$

(13)

3.2. MAXIMUM-SHEAR-STRESS

To determine the ultimate shear stress we use the pressure distribution expressions in the following way. By replacing X by $S \sin$ Equation (12) and substituting the result in Equation (7); afterwards, by replacing X by x/a and S by s/a and integrating over the loaded region, $-1 < S < 1$, we get the next dimensionless stress equations:

$$\frac{\sigma_x}{p_0} = -\frac{2Z}{\pi} \int_{-1}^1 \frac{(1-S^2)^{1/2} (x-s)^2 ds}{[(x-s)^2 + z^2]^2}$$

$$\frac{\sigma_z}{p_0} = -\frac{2z^3}{\pi} \int_{-1}^1 \frac{(1-S^2)^{1/2} ds}{[(x-s)^2 + z^2]^2}$$

(14)

$$\frac{\tau_{zx}}{p_0} = -\frac{2z^2}{\pi} \int_{-a}^a \frac{(1-S^2)^{1/2} (x-s) ds}{[(x-s)^2 + z^2]^2}$$

(15)

$$\frac{\tau}{p_0} = \frac{|\sigma_1 - \sigma_2|}{2}$$

(16)

Equations (14) are the equations allowing determining the stresses in each point inside the gear tooth when the pressure distribution $p(s)$ is applied. Maximum dimensionless shear stress values, τ/p_0 , at some points of the gear tooth contact surface into the region $-1 < X < 1$ and $0 < Z < 1.5$. After applying limits it is clear that $\tau/p_0 = 0.3$ is the maximum dimensionless shear stress and it is located at $Z = 0.8$ beneath the gear tooth work surface. By applying the Tresca yield criterion [13], the maximum pressure to reach this shear stress level is:

$$p_0 = \frac{\tau}{0.3} = \frac{\sigma_{max}}{(2)(0.3)} = 1.66\sigma_{max}$$

(17)

where σ_{max} is the maximum normal stress of material.

Equation (17) can be rewritten in terms of load per unit length P using Equation (11), which results in

$$\sigma_{max} = \frac{2P}{1.66\pi a}$$

(13)

3.3. SURFACE STRESS EQUATION WITH THE GEAR PARAMETERS

Introducing the gear parameters into the surface stress equation we make use of the next relationship

$$P = \frac{W}{b}$$

Where W is the total load applied and b the tooth face width; then, substituting P in Equation (13), we have

$$\frac{\sigma_x}{p_0} = -\frac{2Z}{\pi} \int_{-1}^1 \frac{(1-S^2)^{1/2} (x-s)^2 ds}{[(x-s)^2 + z^2]^2}$$

(14)

On the other hand, the equivalent radius of tooth gear is a function of the pinion and gear tooth curvature radii. Then

$$\rho_p = R_1$$

(15)

$$\rho_g = R_2$$

Where ρ_p is the pinion pitch radius, C is the centre distance and ϕ the pressure angle. Then, substituting Equations (15) into Equation (3), we have,

$$\frac{1}{R} = \left(\frac{1}{R_1} + \frac{1}{R_2} \right) = \left(\frac{1}{\rho_p} + \frac{1}{\rho_g} \right)$$

(16)

Finally, combining Equations (10.1), (14) and (16), it can be found that,

$$\sigma_{max} = \sqrt{\frac{E \times W}{1.66^2 \pi b} \left(\frac{1}{\rho_p} + \frac{1}{\rho_g} \right)}$$

(17)

This is the equation called Gear Design Equation is used to calculate the surface stresses as

function of the gear parameters and the maximum shear stress, responsible of material failure. In gear manufacturing this max.stress must always be smaller than the material yield stress σ_y .

$$\sigma_{\max} < \sigma_y \quad (18)$$

5. CONCLUSION

The performed investigation allows making the following conclusion:

Design of worm and worm gear pair for plug valve application is developed.

Also, Gear design equation for calculating the surface stress for gear and maximum shear-stress, which is responsible for the gear material failure is developed

REFERENCES

1. Su, D. and Qin, D., 2003. Integration of numerical analysis, virtual simulation and finite element analysis for the optimum design of worm gearing. *Journal of Materials Processing Technology*, 138(1), pp.429-435.
2. Yeh, T.J. and Wu, F.K., 2009. Modeling and robust control of worm-gear driven systems. *Simulation Modelling Practice and Theory*, 17(5), pp.767-777
3. Ankush, R.D. and Darade, P.D., 1908. Design and analysis of Worm pair used in Self-locking system with development of Manual Clutch.
4. Litvin, F.L., Gonzalez-Perez, I, Yukishima, K., Fuentes, A. and Hayasaka, K., 2007. Design, simulation of meshing, and contact stresses for an improved worm gear drive. *Mechanism and Machine Theory*, 42(8), pp.940-959.
5. Boantă, C.I. and Boloş, V., 2014. The Mathematical Model of Generating Kinematic for the Worm Face Gear with Modified Geometry. *Procedia Technology*, 12, pp.442-447.
6. Wang, J., Kong, L., Liu, B., Hu, X., Yu, X. and Kong, W., 2014. The mathematical model of spiral bevel gears-A review. *Strojnikivestnik- Journal of Mechanical Engineering*, 60(2), pp.93-105.
7. BhosaleKailash, C. and Dongare, A.D., Photoelastic Analysis of Bending Strength of Helical Gear. *Innovative Systems Design and Engineering*, ISSN, pp.2222-1727.
8. Hinojosa-Torres, J., Hernández-Anda, J.L. and Aceves-Hernández, J.M., 2010. Mathematical model to determine the surface stress acting on the tooth of gear. *Theoretical and Applied Mechanics*, 37(2), pp.97-110.
9. Özgüven, H.N. and Houser, D.R., 1988. Mathematical models used in gear dynamics—a review. *Journal of sound and vibration*, 121(3), pp.383-411.
10. Maitra G.M. (2014), „Hand Book of Gear Design" , Tata McGraw-Hill Publishing Company Limited, New Delhi, 2nd edition.
11. Shigley, J.E. and Mischke, C.R., 1989. *Mechanical Engineering Design*, Fifth Edition, McGraw-Hill, Inc, 1989,
12. Timoshenko, S., Timoshenko, S. and Goodier, J.N., 1951. *Theory of Elasticity*, by S. Timoshenko and JN Goodier,
13. McGraw-Hill book Dieter, G.E., 2005. *Mechanical metallurgy*, 1988, SI metric edition.